Materials Research. 2018; 21(1): e20170387
DOI: http://dx.doi.org/10.1590/1980-5373-MR-2017-0387

Microstructure and Properties of Cu-ZrO_2 Nanocomposites Synthesized by in Situ Processing

Marwa Elmahdy[a]*, Gamal Abouelmagd[b], Asaad Abd Elnaeem Mazen[b]

[a]Mechanical Department, Higher Technological Institute, 10th Of Ramadan City, P.O. Box 228, Sharqia, Egypt
[b]Production Engineering and Design Department, Faculty of Engineering, Minia University, Minia, Egypt

Received: April 19, 2017; Revised: August 20, 2017; Accepted: September 17, 2017

In situ chemical reaction method was used to synthesize Cu-ZrO_2 nanocomposite powders. The process was carried out by addition of $NH_4(OH)$ to certain amount of dispersed $Cu(NO_3)_2 \cdot 3H_2O$ and $ZrOCl_2 \cdot 8H_2O$ solution. Afterwards, a thermal treatment at 650 °C for 1 h was conducted to get the powders of CuO and ZrO_2 and remove the remaining liquid. The CuO was then reduced in preferential hydrogen atmosphere into copper. The powders were cold pressed at a pressure of 600 MPa and sintered in a hydrogen atmosphere at 950 °C for 2 h. The structure and characteristics were examined by X-ray diffraction (XRD), field emission scanning electron microscopy (FESEM) and transmission electron microscopy (TEM). The results showed that the nanosized ZrO_2 particles (with a diameter of about 30-50 nm) was successfully formed and dispersed within the copper matrix. The density, electrical conductivity, mechanical strength measurements (compression strength and Vickers microhardness) and wear properties of Cu-ZrO_2 nanocomposite were investigated. Increment in the weight % of ZrO_2 nano-particles up to 10 wt.% in the samples, caused the reduction in the densification (7.2%) and electrical conductivity (53.8%) of the nanocomposites. The highest microhardness (146.5 HV) and compressive strength (474.5 MPa) of the nanocomposites is related to the Cu-10 wt.% ZrO_2. Owing to the good interfacial bonding between uniformly dispersed ZrO_2 nanoparticles and the copper matrix. The abrasive wear rate of the Cu-ZrO_2 nanocomposite increased with the increasing load or sliding velocity and is always lower than that of copper at any load or any velocity.

Keywords: *Cu-ZrO_2 nanocomposite, In Situ chemical synthesis, Microhardness, Compressive strength, Electrical conductivity, Abrasive wear*

1. Introduction

Nano-sized ceramic particles in a nanocrystalline metal matrix prepared by the in situ chemical reaction can improve the mechanical, tribological, and anti-corrosion properties of the metal[1-5]. In recent years nanocomposite materials have attracted much attention owing to their improved physical and mechanical properties. The properties of such materials strongly depend on the particle size and distribution of nanoparticles in the matrix[6-9].

Copper based materials are widely used where high electrical and thermal conductivities are required. Rotating source neutron targets, combustion chamber liners, the electrode of resistance welding, integrated circuit sealing materials, high voltage switches and heat exchangers are examples of copper based materials' applications. These applications require a suitable performance, e.g. high conductivity and excellent mechanical properties, at elevated temperatures and in electronic industries[10-14]. Pure copper, on the other hand, suffers from low tensile strength, low hardness and poor wear resistance[10,12,15]. Therefore, one of the potential solutions for these drawbacks is the incorporation of a reinforcement element, which results in copper matrix composite as a by-product[16-18].

Oxide dispersion strengthening (ODS) is a suitable method to improve the mechanical properties of the copper matrix composites[19]. Due to high interfacial energy between the molten metal and oxide particles melting and casting techniques are not used to fabricate such composites; therefore these composites should be produced by the powder metallurgy methods. The main steps of these methods are the production of composite powder, followed by consolidation to get a bulk material.

The oxide dispersoids can be added into the copper matrix by ex-situ method or in-situ method. The shortcoming of ex-situ method is that nano-sized oxide dispersoids can be homogeneously dispersed in the copper matrix[20]. Meanwhile, the bonding between the particles and the copper matrix is poor. In contrast, dispersion strengthened copper alloys can be produced by various in-situ processing methods with a homogeneous structure, such as internal oxidation, reactive spray deposition and reaction synthesis, etc[20-22].

Nowadays, it is well known that by proper reinforcement selection, better properties for MMCs could be produced.

*e-mail: marwa_Elmahdy2010@yahoo.com.

Considering this comment, a variety of particulate ceramic materials like Al_2O_3[2,6,8,14-16,19-22], SiC[12,13], and TiB_2[18] have been utilized to reinforce the copper matrix. The usage of above reinforcements has led to the enhancement of mechanical properties, which have been reported by researchers cited above. Among these, however, fine stabilized ZrO_2 ceramic particles could be a proper reinforcing material due to their high strength and stiffness, high melting temperature, and relatively good electrical property[23].

Few studies have been published about strengthening copper using zirconia particles by the method of the in-situ chemical reaction. A Cu-ZrO_2 nanocomposite has been prepared by Ding Jian[24] by the in-situ chemical method, and another by Gao Jing[25] using the powder metallurgy techniques, respectively. They studied the effect of the process parameters including the initial pressure, the sintering temperature and sintering time, content of ZrO_2 particles on the properties of the composite.

Based on the above research work, the present study aims at producing homogeneous Cu-ZrO_2 composites from chemically prepared CuO-ZrO_2 mixtures and investigate the effect of ZrO_2 on the crystallite size, particle size and morphology of the obtained powder. Furthermore, their effect on microstructure, and relative density of sintered compacted samples were studied. Electrical conductivity, mechanical and abrasive wear properties of resulting nanocomposites were also studied.

2. Experimental Work

Soluble nitrates of copper (II) nitrate $Cu(NO_3)_2 \cdot 3H_2O$, zirconium oxychloride $ZrOCl_2 \cdot 8H_2O$ and ammonium hydroxide $NH_4(OH)$, could be used as transient components for the in situ chemical synthesis of nanocomposite Cu-ZrO_2 powders. The accomplished in situ chemical processes were adopted to prepare Cu-ZrO_2 nanocomposite, as summarized in Figure 1. This process consists of four main stages:

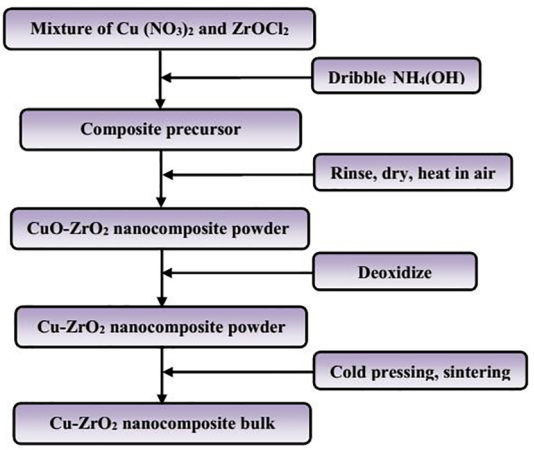

Figure 1. Flowchart of preparation of Cu-ZrO_2 nanocomposite powder using in situ chemical process.

- Making an aqueous solution of $Cu(NO_3)_2 \cdot 3H_2O$ and $ZrOCl_2 \cdot 8H_2O$; the quantities of salts were taken such that the resulting composition of the Cu-ZrO_2 nanocomposite system with 2.5, 5 &10 wt. % of zirconia would be attained;
- $NH_4(OH)$, dissolved in water (28%), was added dropwise while stirring the mixture with a magnetic stirrer for 20 min and then washed with water repeatedly and filtered Eqn. (1);

$$Cu(NO_3)_2 + ZrOCl_2 + 3NH_4(OH) + H_2O \rightarrow Cu(OH)_2 + Zr(OH)_3 + 2NH_4NO_3 + NH_4Cl_2 \quad (1)$$

- The filtered mixture was dried at 120 °C overnight, and then annealed in an air atmosphere at 650 ◦C for 1 h to obtain the composite powder of the Cu and Zr oxides Eqn. (2);

$$Cu(OH)_2 + Zr(OH)_3 \xrightarrow{650\,^{\circ}C,\,1h} CuO + ZrO_2 + 2H_2O + \frac{1}{2}O_2 \quad (2)$$

- Reduction of thermally treated powders in a hydrogen atmosphere at a temperature of 500 °C for one hour, whereby the copper oxide was transformed into elementary copper and the ZrO_2 remained unchanged Eqn. (3).

$$CuO + ZrO_2 \xrightarrow{500\,^{\circ}C,\,30\ \mathrm{min}} Cu + ZrO_2 + H_2O \quad (3)$$

After reduction, the powders were characterized by X-ray diffraction (XRD) with CuKα radiation, λ= 1.5418 Å and at 36 kV and 26 mA. The X-ray data were collected in steps of 0.02° (2θ) with the scanning scope of 20-80°. Evaluation of effective sizes of coherent scattering area was carried out in compliance with the Scherrer formula with the strongest peaks of phases analyzed. And the zirconia extracted from the Cu-ZrO_2 composite powder was characterized using transmission electron microscopy (TEM; Model JEOL JEM-2010).

Prior to sintering, the produced Cu-ZrO_2 nanocomposite powders were compacted in a hydraulic press at a pressure of 600 MPa. in a steel mold to obtain cylindrical shaped specimens having 12 mm diameter and 12 mm height. The powders were mixed with 0.5% paraffin wax as a lubricant to reduce friction during compaction. Sintering of all the green compacts were carried out using a ceramic tubular furnace in a hydrogen atmosphere at 950 °C for 2 h and a heating rate of 10 °C /min[21].

The microstructure of the prepared nanocomposites was examined by optical microscope model Olympus PMG 3−F3, while microstructural analyses were performed using field emission scanning electron microscopy (FESEM Hitachi

S4160) and SEM fitted with EDS. True densities of the nanocomposites were measured by using the Archimedes' method (ASTM-C20) and compared with the theoretical densities to obtain varying degree of densification. The theoretical densities of compacts were calculated from the simple rule of mixtures, taking the fully dense values for copper (8.96 g/cm^3) and zirconia (5.68 g/cm^3). The electrical resistivity of the composite samples was measured using the two-probe using Omega micro-ohmmeter, and electrical conductivity of composite was calculated from these measurements. Vickers microhardness was performed on the polished samples under a test load of 50 g_f and a dwell time of 10 s in accordance with the ASTM standard E 92. In order to obtain optimum results, microhardness values were determined by taking the average of six different measurements randomly on each sample. The Compression tests were performed over an initial strain rate of 10^{-4} s^{-1} at room temperature using a universal testing machine model HU−F500KN. Cylindrical specimens with a height of 12 mm and a diameter of 12 mm were used in compliance with ASTM E9-89a standard for measuring the compressive response of the matrix and composite materials[26]. Special graphite based grease is placed between the tested specimen and the platen of the compression machine to minimize friction. The percentage reduction was maintained at 60 %. The end surfaces of the specimen were maintained as normal to the axis of specimen.

Abrasive wear tests were carried out with a pin-on-disc tester. Rectangular specimens having contact area of 44 mm^2 are loaded against a rotating disc, which carried a bonded abrasive SiC paper of 600 grit. The applied normal loads used were 3, 5, 7 and 9 N. The sliding velocities employed were 0.5, 0.75 and 1 m/s. The sliding distance was kept constant at 120 m for each sample. In these tests, each specimen was ground up to grade 2000 abrasive paper to ensure that the wear surface is in complete contact with the abrasive counterface. The weight loss of the pin was measured at various intervals in an analytical balance of 0.0001g precision. The pins were cleaned in acetone and dried prior to each weight measurement. The abrasive wear rate of the pins was defined as the weight loss suffered per unit sliding distance.

3. Results and Discussions

3.1 Characterization of the prepared powders

Figure 2 shows X-ray diffraction (XRD) pattern of nanocomposite (Cu-2.5, 5 and 10 wt.% ZrO_2) powders after reduction by hydrogen. The sharp XRD peaks on the pattern correspond to Cu phase and the low intensity ones could be attributed to tetragonal ZrO_2 phase. The ZrO_2 peaks showed lower intensity values than that of copper. It was noticed that the intensity of the ZrO_2 peaks are not clear up to 10%

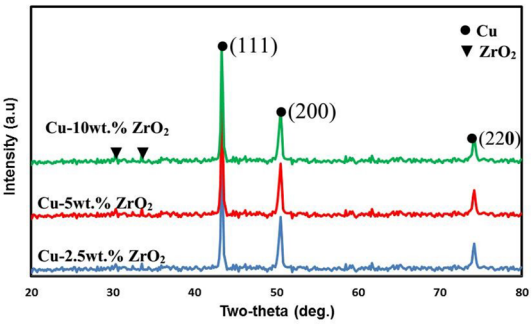

Figure 2. XRD pattern of the Cu-ZrO_2 nanocomposite after reduction.

ZrO_2. This may be attributed to the fact that ZrO_2 particles are extremely small that they were embedded in the copper matrix. However, XRD peak intensities of the ZrO_2 phase are noticeably increased with increasing weight percentage of ZrO_2. The particle size of zirconia was calculated from X-ray line broadening using Scherer's formula ($D = 0.9\lambda/\beta \cos\theta$), where, D is the crystallite size, λ is the wavelength of the radiation, θ is the Bragg's angle and β is the full width at half maximum[27]. The crystallite size of zirconia nanoparticles showed a value of 50 nm whilst size of copper crystallites were 270 nm.

The obtained Cu-ZrO_2 nanocomposite powders were characterized by FESEM as presented in Figure 3. Particles with a size of 20-60 nm are clearly visible, as well as the presence of few agglomerates >100 nm. The particles are irregularly shaped, with the presence of individual nodular particles with a rough surface morphology.

The structure of ZrO_2 is formed during the heat treatment of nanocomposite powder in air (650 °C, 1 h). In order to identify the ZrO_2 dispersoids embedded in Cu-ZrO_2 powders, mixed powder was flushed with 10% nitric acid to selectively pickle Cu matrix, the remaining ZrO_2 dispersions were collected by filtering. Figure 4 shows the particle sizes and shapes of ZrO_2 powder. This was observed clearly in the high resolution of TEM. TEM observations confirmed that the ZrO_2 particle size ranged from 40 to 60 nm. All extracted particles showed regular shape appearance.

3.2 Characterization of the sintered nanocomposites

Microstructural studies conducted on the composites revealed homogeneous distribution of the ZrO_2 particles in the Cu matrix. To achieve optimized mechanical and electrical properties of the composite materials, it is significant to obtain uniform distribution of reinforcement in the matrix. If reinforcement particles in the composites do not disperse uniformly, this affects mechanical and electrical properties of composites negatively[23]. Microstructural morphology and distribution of the components in the Cu ZrO_2 composites sintered at 950 °C for 2 h, as a function of ZrO_2 content,

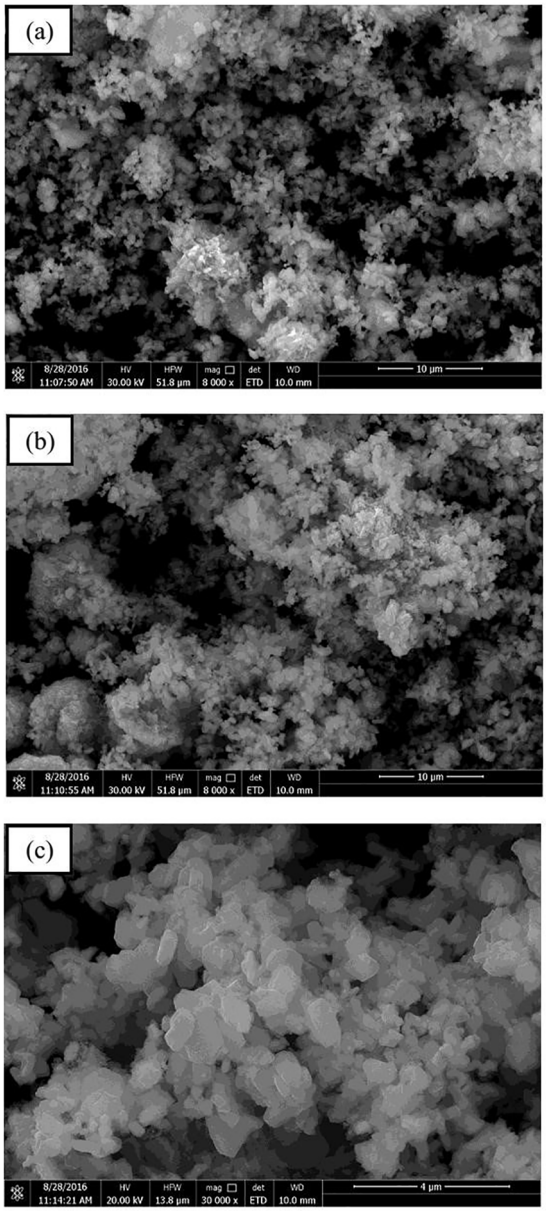

Figure 3. FE-SEM micrograph of the nanocomposite powder; (a) Cu-2.5 wt% ZrO_2, (b) Cu-5 wt% ZrO_2 and (c) Cu-10 wt% ZrO_2.

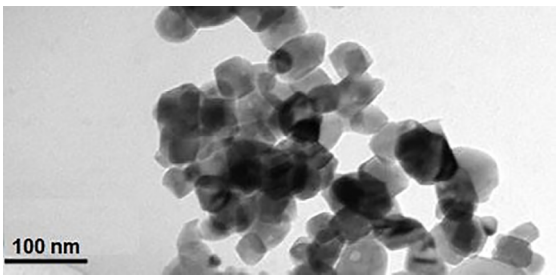

Figure 4. TEM images of ZrO_2 extracted from the Cu-ZrO_2 nanocomposite powder.

are shown in Figure 5. Brighter regions imply Cu matrix and darker and cornered particles imply the reinforcement component of ZrO_2. It can be seen that ZrO_2 particles are homogeneously dispersed in the Cu matrix.

Figure 6 shows the FE-SEM images of Cu-2.5, 5 and 10 wt.% ZrO_2 composites sintered at 950 ° C for 2 h. The FE-SEM micrographs give abundant information about the ZrO_2 distribution, status of physical intimacy between Cu and ZrO_2 and mechanical phenomena. With the increase in weight percentage of ZrO_2 in Cu matrix the efficiency of distribution becomes remarkably better. The density difference between the matrix and reinforcement also leads to the formation of clusters sometimes at high wt.% of the reinforcement[28]. The physical contact of the ZrO_2 nanoparticles with the Cu matrix can be attributed to the high atomic diffusivity of the nanoparticles. The stabilization of the surface energy of nanoparticles is a thermodynamic driven phenomenon; hence it is quite obvious that the physical adherence of Cu with ZrO_2 is proper in the nanocomposites.

In order to determine the distribution of elements in the structure, surface analysis of the sample was performed by FE-SEM and the composition scanning (EDS) images shown in Figure 7. From the microstructure analysis, it can be concluded that the samples are well densified and sintered. Peaks of elementary Cu, O and Zr were detected, which are related to the composition of ZrO_2 particles and Cu matrix, respectively. The ZrO_2 particles with the high melting point, high hardness and excellent thermal stability and chemical inertness do not melt or coarsen when the annealing temperature approaches the melting point of copper, which effectively pins down the grain and sub-grain boundaries of the copper matrix and impedes the movement of dislocation and improves strength of the composite at elevated temperature.

The powder compaction is an important step in the preparation of bulk materials by powder technology. This step controls the porosity and the shape of the final product that can be sintered. Bar graph illustrating the densification measured after compaction and sintering of the Cu-ZrO_2 composites as a function of ZrO_2 content is shown in Figure 8. Relative density is the ratio of experimental and theoretical densities of sample. Experimental density was determined by the Archimedes method and the theoretical density was calculated from the simple rule of mixtures. It was clear that, the densification of Cu-ZrO_2 composites was decreased from 95.6 % to 88.7 % by increasing ZrO_2 weight fraction from 0 % up to 10% under the same processing conditions. This is due to the density of ZrO_2 nanoparticles being much smaller than that of copper and high porosity content which accompanies the high fraction of reinforcement ZrO_2[24]. Moreover, decreasing of relative density with increasing zirconia content in the metal matrix probably could be due

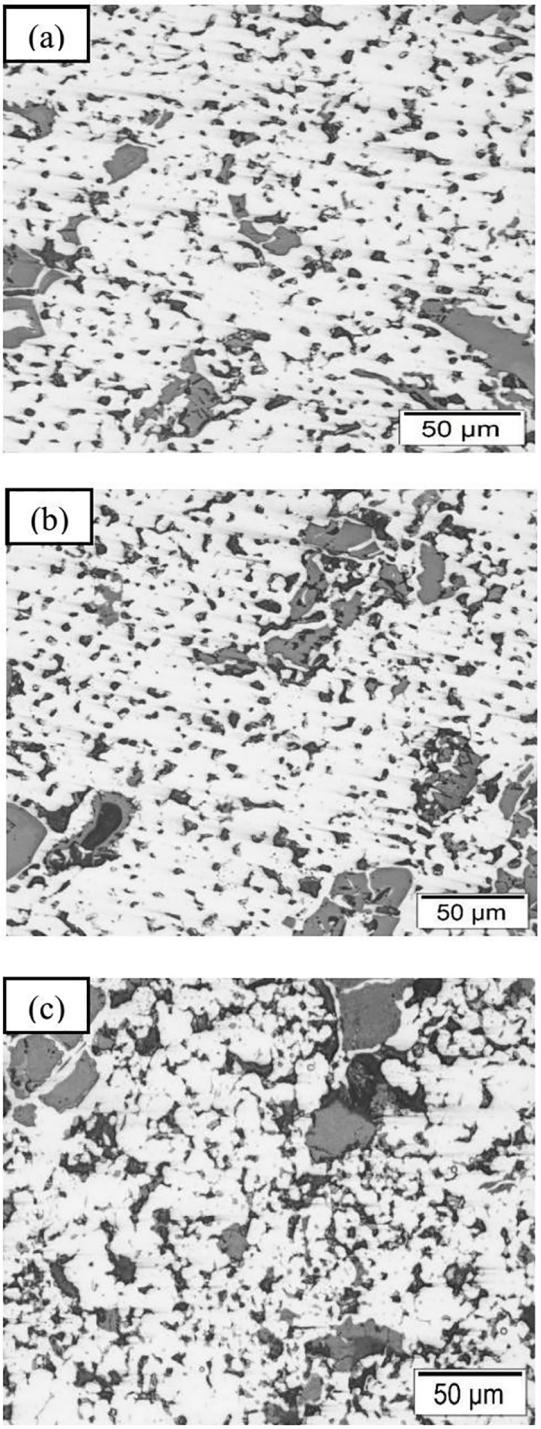

Figure 5. Optical images of the nanocomposite metallographic structure; (a) Cu-2.5 wt% ZrO_2, (b) Cu-5 wt% ZrO_2 and (c) Cu-10 wt% ZrO_2.

to the presence of zirconia nanoparticles on the surface of copper micrometric particles produces a remarkable increase of porosity in the microstructure of the samples. The creation of voids in the Cu matrix hinders the densification and impedes the continuity in intimacy contact of Cu and

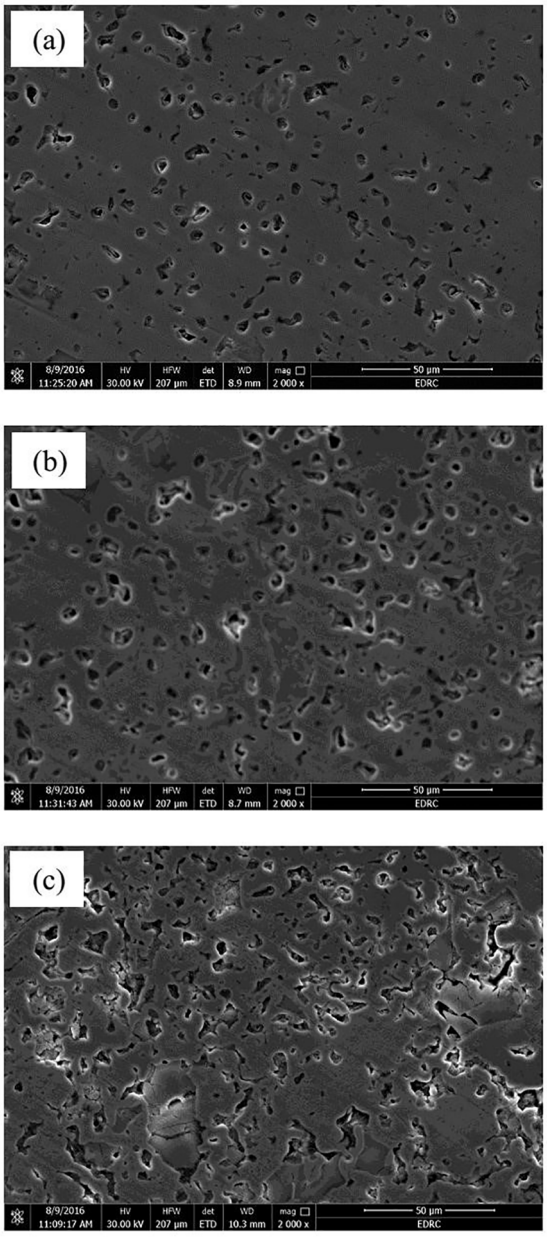

Figure 6. FE-SEM micrographs of nanocomposites; (a) Cu-2.5 wt% ZrO_2, (b) Cu-5 wt% ZrO_2 and (c) Cu-10 wt% ZrO_2.

zirconia. In addition, the decline in the pressing capacity of samples with increasing in the amount of ZrO_2 is due to the high hardness of ZrO_2. Therefore, these composites have lower compressibility that results in lower densification[29,30].

Electrical conductivity of each sample was measured and compared to the value of standard electrical conductivity, which is given by copper compact of industrial grade and reported as percentage of standard conductivity as shown in Eq. (4);

$$\text{Electrical conductivity (\% std)} = \frac{\sigma_s}{\sigma_{std}} \text{x} 100 \qquad (4)$$

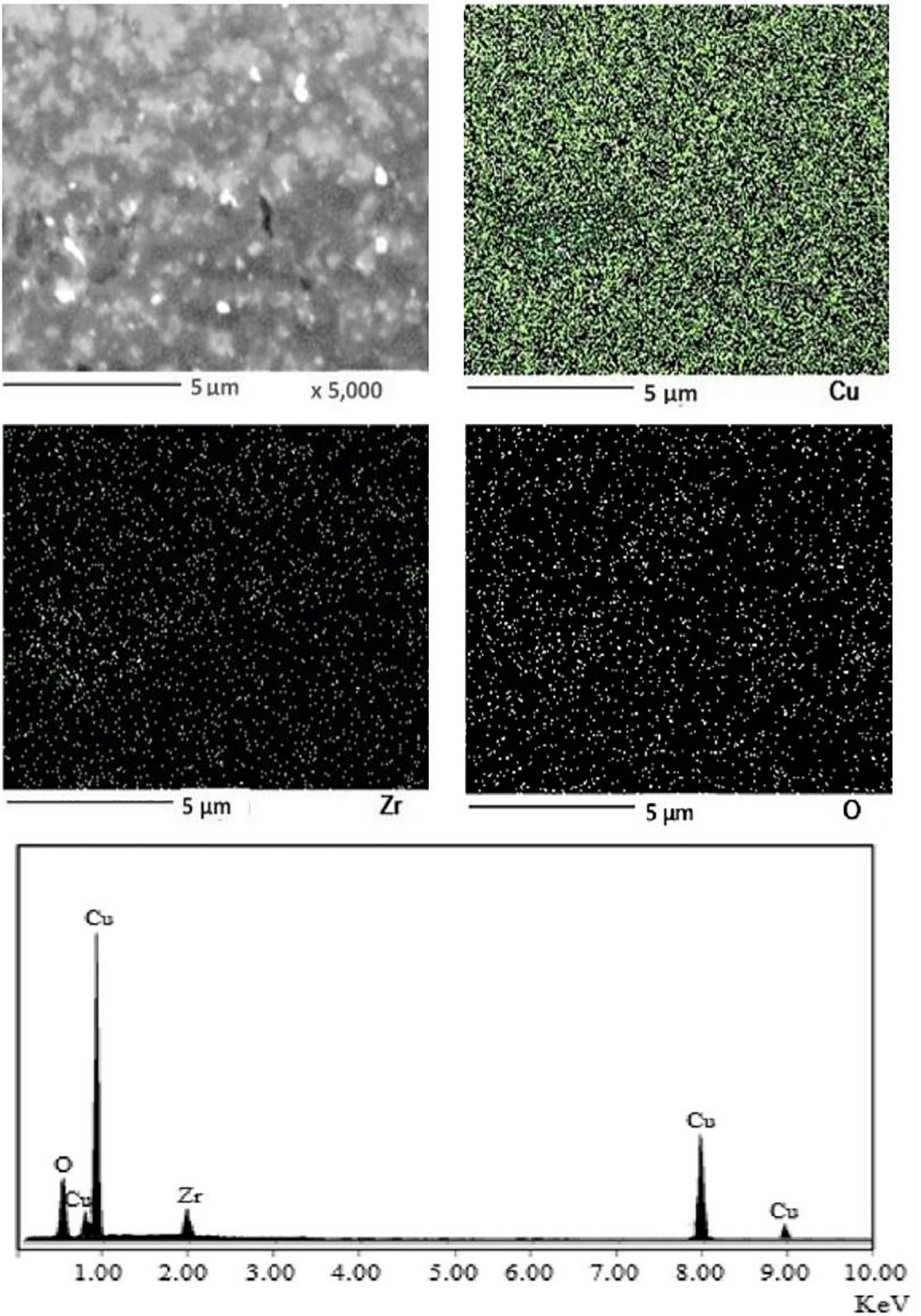

Figure 7. FE-SEM micrograph (a) and EDS (b) of Cu-10 wt.% ZrO_2 nanocomposite.

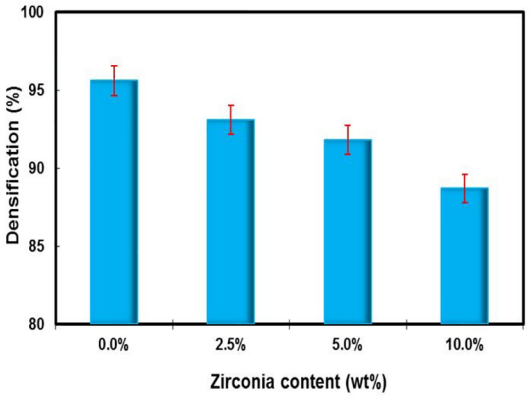

Figure 8. Bar graph of densification of Cu−ZrO_2 composites as function of ZrO_2 content.

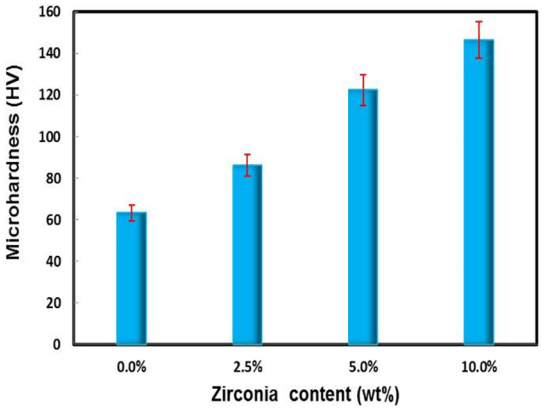

Figure 10. Bar graph of microhardness of Cu−ZrO_2 composites as function of ZrO_2 content.

where σ_s is the electrical conductivity of the tested sample and σ_{std} is the electrical conductivity of the standard copper. Bar graph illustrating the electrical conductivity after compaction and sintering of the Cu-ZrO_2 composites as a function of ZrO_2 content is shown in Figure 9. Electrical conductivity of composites decreased with increasing content of ZrO_2. This can be attributed to the lower electrical conductivity of ZrO_2 compared to that of Cu. The second reason is the agglomeration of some ZrO_2 particles at the grain boundaries which can form a kind of grain boundary phase that increases the scattering of the charge carrier, hence reducing the electrical conductivity. Electrical conductivity of the metal is mainly dependent on the movement of the internal electron. ZrO_2 particles can increase the scattering surfaces for the conduction electrons in the matrix and reduce the electrical conductivity of the Cu matrix composites[31]. Overall, increment in the weight % of ZrO_2 nano-particles up to 10 wt.% in the samples, caused the reduction in the electrical conductivity (53.8%) of the nanocomposites, while using Al_2O_3 decreased the electrical conductivity to18.5%[22].

Bar graph illustrating the microhardness after compaction and sintering of the Cu ZrO_2 composites as a function of ZrO_2 content is shown in Figure 10. It was observed from the present study that by increasing the amount of ZrO_2 from 0% to 10%, microhardness increased from 63.2 to 146.5 HV. The microhardness of Cu is improved considerably with the addition of ZrO_2 nanoparticles at the expense of its ductility, this can be attributed to the high hardness of ZrO_2. The increase in hardness of the composite can also be attributed to the gradual decrease in grain size of the Cu matrix as a result of the presence of nano-ZrO_2 particles. Also, the nano-ZrO_2 particles embedded in the Cu matrix would prevent the slip of the grain boundary of Cu matrix, thereby, improving the hardness of the composite[32]. The hardness of material is a physical parameter indicating the ability of resisting local plastic deformation. Reinforcing nano-ZrO_2 particles with high hardness, are dispersed in the copper matrix and act as obstacles to the movement of dislocation when plastic deformation occurs. Also the hardness enhancement is an indication of high interfacial strength at Cu-ZrO_2 interface and homogeneous distribution of ZrO_2 within Cu matrix[25].

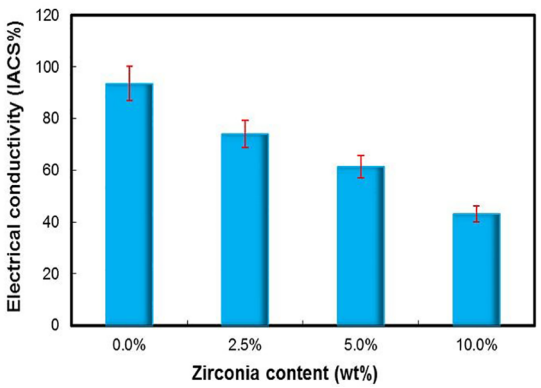

Figure 9. Bar graph of electrical conductivity of Cu−ZrO_2 composites as function of ZrO_2 content.

Bar graph illustrating the compressive strength after compaction and sintering of the Cu-ZrO_2 composites as a function of ZrO_2 content is shown in Figure 11. Obviously, the compressive strength value of Cu-ZrO_2 composite is significantly higher than that of the Cu matrix, suggesting that the ZrO_2 nanoparticles can strongly enhance the mechanical strength of the Cu matrix. The highest value of the compressive strength of the sintered samples, 474.5 MPa, were obtained after addition of up to 10 wt.% ZrO_2. Although tensile testing can determine if a proper bonding has been produced yet, compression test can also be helpful to studying the barreling and upsetting behavior of the compacts. Stronger bonds among particles delay the crack initiation during deformation especially at the time of barreling[33,34].

Also, it can be observed that by increasing the amount of ZrO_2 from 0 to 10 wt.%, the compressive strength increased from 318.7 to 474.5 MPa. This increase can be explained by the presence of incoherent zirconia nanoparticles that act like barriers to the motion of dislocations. Also the compressive

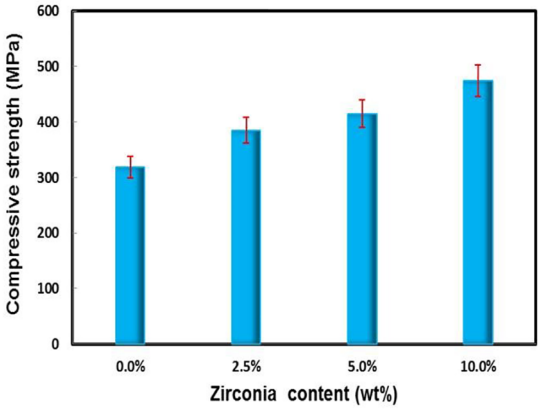

Figure 11. Bar graph of compressive strength of Cu−ZrO_2 composites as function of ZrO_2 content.

strength enhancement is an indication of stronger bonding at Cu-ZrO_2 interface and homogeneous distribution of ZrO_2 within Cu matrix[35]. Additionally, increasing the amount of ZrO_2 lead to a decrease in the distance between the ZrO_2 particles. Decreasing the distance between the ZrO_2 particles will increase the required tension for dislocation motion between the ZrO_2 particles leading to an increase in the material strength[31].

The fractographs of different deformed composites at room temperature are shown in Figure 12. It was observed that the shape of compression specimens gradually changed their original shapes from cylinder to barrel-like shape during the deformation due to friction between the surfaces of the specimens and graphite plates. It was observed during the compression tests that, all tested nanocomposite specimens

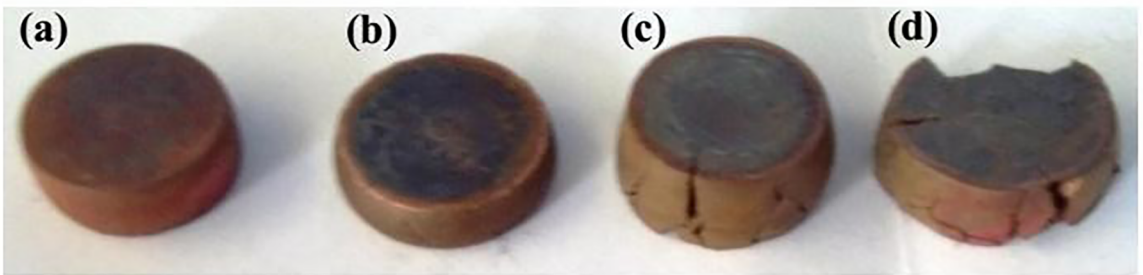

Figure 12. Fractography of different deformed composites: (a) Cu, (b) Cu-2.5 wt.% ZrO_2, (c) Cu-5 wt.% ZrO_2, (d) Cu-10 wt.% ZrO_2.

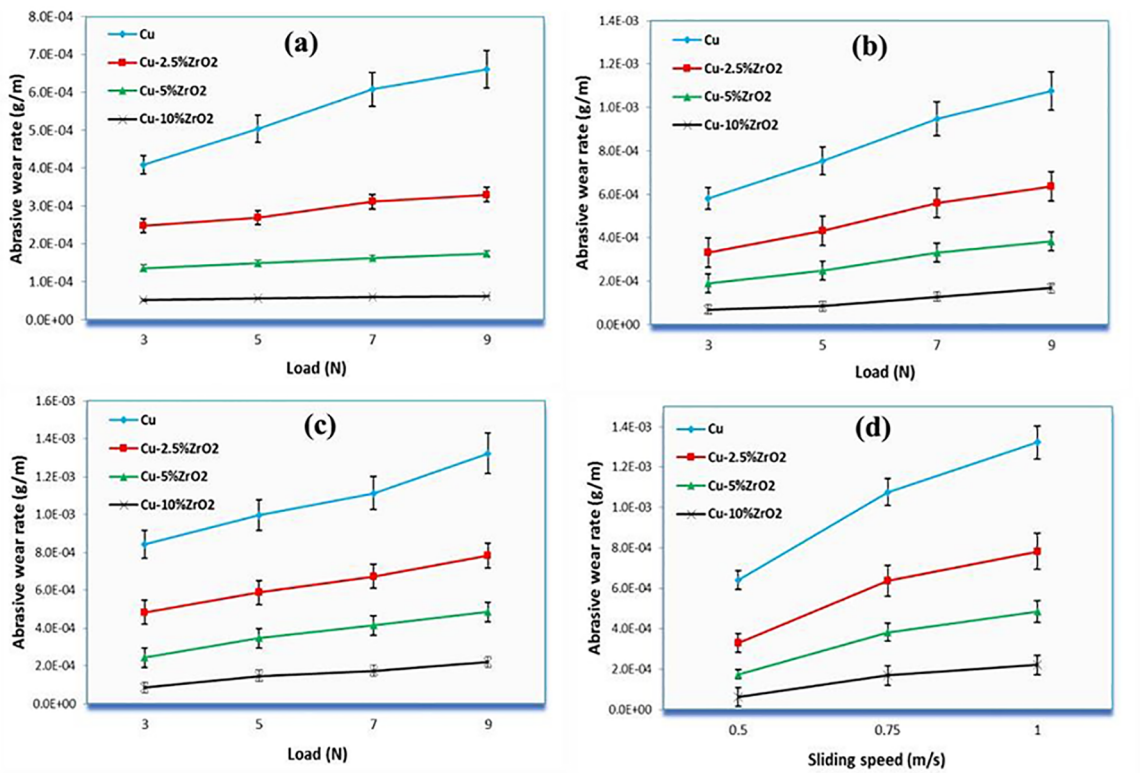

Figure 13. Abrasive wear rate of Cu−ZrO_2 nanocomposites with various ZrO_2 content at the sliding distance of 120 m; (a) V = 0.5 m/s, (b) V = 0.75m/s, (c) V = 1 m/s, (d) load = 9 N.

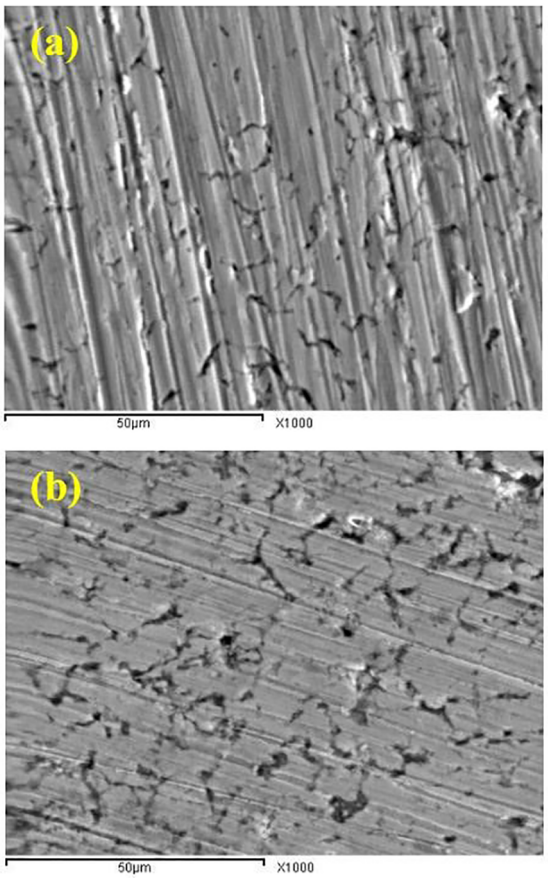

Figure 14. The worn surface; (a) Cu matrix, (b) Cu-10 wt. % ZrO_2 nanocomposites.

were cracked before reaching 60% reduction in height whilst monolithic copper specimen showed no cracks up to 60% reduction. It was observed that increasing ZrO_2 content composites are more prone to circumferential cracks.

Figures 13(a-c) show the effect of the applied load on abrasive wear rate of Cu ZrO_2 nanocomposite at sliding distance of 120 m and various velocities from 0.5 to 1 m/s. It can be observed from Figs. 13(a-c), that with increasing the applied normal load during wear tests, the abrasive wear rate of pure copper and Cu-ZrO_2 nanocomposite increases[20,21]. Applied load affects the wear rate of compacts significantly and is the most dominating factor controlling the wear behavior. By increasing the applied load, plastic deformation on the subsurface due to increased penetration depth of counterface can occur.

It can also be seen that the increase in amount of incorporated ZrO_2 particles in the pure copper matrix decreased the abrasive wear rate and increased the wear resistance. The significant reduction in the abrasive wear rate of Cu-ZrO_2 nanocomposite is due to the incorporation of inert ZrO_2 nanoparticles in the pure copper matrix which led to reduction in the size of copper crystals and an improvement in microhardness of the nanocomposites. This latter is due to the combined effect of both grain-refinement and dispersion-strengthening, which results in considerable improvement in abrasion wear resistance of the Cu-ZrO_2 nanocomposites[36,37]. It can also be clearly seen in Figure 13d that the abrasive wear rate increases with the increase of sliding velocity. This is associated with the increase of surface temperature under high sliding velocity, which promotes softening of the surface, leading to more surface and subsurface damage, eventually resulting in higher abrasive wear rate.

The worn surfaces of unreinforced Cu and Cu−10% ZrO_2 nanocomposite specimens under 9 N load and sliding velocity of 1 m/s were revealed in Figure 14. As shown in Figure 10a, the continuous furrow and deeper furrow can be found on the surface, which was paralleled to sliding direction. Some finer copper grains had peeled off during the wear process. The worn surface of the Cu-10% ZrO_2 nanocomposites was shown in Figure 10b. Compared with Cu matrix materials, the shallower and narrower furrow was found on the wear surface, and grain stripping was slight. The figure shows distinct grooves and ridges running parallel to each other's in the sliding direction. It can be seen from the micrographs that the grooves are wider and debris in Cu matrix as compared within the Cu-ZrO_2 one under the sample conditions indicating the higher wear resistance of Cu-ZrO_2 sample. This can be explained by the formation of a thick transfer lager which protects the underlying Cu matrix from any contact with the sliding SiC abrasive counterpart so reduction of wear rate takes place.

4. Conclusions

The following conclusions can be drawn based on the present study:

1. Cu matrix reinforced with different weight fraction of the zirconia (2.5, 5 and 10 wt.%), were successfully prepared by in situ chemical route followed by pressing and sintering.
2. In situ chemical route gave nanoparticles of zirconia of 50 nm size that are uniformly dispersed within Cu-matrix.
3. Increasing the weight fraction of ZrO_2 nano-particles up to 10 wt.% in the samples, caused reduction in the densification (7.2%) and electrical conductivity (53.8%) of the nano-composites.
4. The Cu-10 wt.% ZrO_2, achieved the highest micro-hardness (146.5 HV) and compressive strength (474.5 MPa) of the nanocomposites.
5. The abrasive wear rate of the Cu-ZrO_2 nanocomposite increased with the increasing load or sliding velocity and is always lower than that of unreinforced copper at any load or any velocity. The wear resistance of the Cu-ZrO_2 nanocomposite reinforced with 10% ZrO_2 is obviously improved.

5. References

1. Zhang Z, Wu X, Jiang C, Ma N. Electrodeposition of Ni matrix composite coatings containing ZrC particles. *Surface Engineering.* 2014;30(1):21-25.
2. Wagih A, Fathy A. Experimental investigation and FE simulation of spherical indentation on nano-alumina reinforced copper-matrix composite produced by three different techniques. *Advanced Powder Technology.* 2017;28(8):1954-1965.
3. Jiang JB, Zhang L, Zhong QD, Zhou QY, Wang Y, Luo J. Preparation and characterization of nickel-nano-B_4C composite coatings. *Surface Engineering.* 2012;28(8):612-619.
4. El Mahallawy N, Fathy A, Hassan M. Evaluation of mechanical properties and microstructure of Al/Al-12%Si multilayer via warm accumulative roll bonding process. *Journal of Composite Materials.* 2017.
5. Selvakumar N, Vettivel SC. Thermal, electrical and wear behavior of sintered Cu-W nanocomposite. *Materials & Design.* 2013;46:16-25.
6. Fathy A, Megahed AA. Prediction of abrasive wear rate of in situ Cu-Al_2O_3 nanocomposite using artificial neural networks. *International Journal Advanced Manufacturing Technology.* 2012;62:953-963.
7. Fathy A, Wagih A, El-Hamid MA, Hassan A.A. The effect of Mg add on morphology and mechanical properties of Al-xMg/10Al_2O_3 nanocomposite produced by mechanical alloying. *Advanced Powder Technology.* 2014;25(4):1345-1350.
8. Shehata F, Abdelhameed M, Fathy A, Elmahdy M. Preparation and Characteristics of Cu-Al_2O_3 Nanocomposite. *Open Journal of Metal.* 2011;1(2):25-33.
9. Balasubramanian A, Srikumar DS, Raja G, Saravanan G, Mohan S. Effect of pulse parameter on pulsed electrodeposition of copper on stainless steel. *Surface Engineering.* 2009;25(5):389-392.
10. Akhtar F, Askari SJ, Shah KA, Du X, Guo S. Microstructure, mechanical properties, electrical conductivity and wear behavior of high volume TiC reinforced Cu-matrix composites. *Materials Characterization.* 2009;60(4):327-336.
11. Girish BM, Basawaraj BR, Satish BM, Somashekar DR. Electrical resistivity and mechanical properties of tungsten carbide reinforced copper alloy composites. *International Journal of Composite Materials.* 2012;2(3):37-42.
12. Fathy A, Sadoun A, Abdelhameed M. Effect of matrix/reinforcement particle size ratio (PSR) on the mechanical properties of extruded Al-SiC composites. *The International Journal of Advanced Manufacturing Technology.* 2014;73(5-8):1049-1056.
13. Efe GC, Ipek M, Zeytin S, Bindal C. An investigation of the effect of SiC particle size on Cu-SiC composites. *Composites Part B: Engineering.* 2012;43(4):1813-1822.
14. Shehata F, Fathy A, Abdelhameed M, Moustafa SF. Fabrication of copper-alumina nanocomposites by mechanochemical routes. *Journal of Alloys and Compounds.* 2009;476(1-2):300-305.
15. Ritasalo R, Liua XW, Söderberg O, Keski-Honkola A, Pitkänen V, Hannula SP. The Microstructural Effects on the Mechanical and Thermal Properties of Pulsed Electric Current Sintered Cu-Al_2O_3 Composites. *Procedia Engineering.* 2011;10:124-129.
16. Fathy A, Wagih A, El-Hamid MA, Hassa A. Effect of Mechanical Milling on the Morphology and Structural Evaluation of Al-Al_2O_3 Nanocomposite Powders. *International Journal of Engineering-Transactions A: Basics.* 2013;27(4):625-632.
17. Tsui HP, Hung JC, Wu KL, You JC, Yan BH. Fabrication of a Microtool in Electrophoretic Deposition for Electrochemical Microdrilling and in Situ Micropolishing. *Materials and Manufacturing Processes.* 2011;26(5):740-745.
18. Tu JP, Wang NY, Yang YZ, Qi WX, Liu F, Zhang XB, et al. Preparation and properties of TiB_2 nanoparticle reinforced copper matrix composites by in situ processing. *Materials Letters.* 2002;52(6):448-452.
19. El Mahallawy N, Fathy A, Abdelaziem W, Hassan M. Microstructure evolution and mechanical properties of Al/Al-12%Si multilayer processed by accumulative roll bonding (ARB). *Materials Science and Engineering: A.* 2015;647:127-135.
20. Vieira Junior LE, Bendo T, Nieto MI, Klein AN, Hotza D, Moreno R, et al. Processing of Copper Based Foil Hardened with Zirconia by Non-Deformation Method. *Materials Research.* 2017;20(3):835-842.
21. Shehata F, Fathy A, Abdelhameed M, Moustafa SF. Preparation and properties of Al_2O_3 nanoparticle reinforced copper matrix composites by in situ processing. *Materials & Design.* 2009;30(7):2756-2762.
22. Fathy A, Shehata F, Abdelhameed M, Elmahdy M. Compressive and wear resistance of nanometric alumina reinforced copper matrix composites. *Materials & Design.* 2012;36:100-107.
23. Fathy A, Elkady O, Abu-Oqail A. Production and properties of Cu-ZrO_2 nanocomposites. *Journal of Composite Materials.* 2017.
24. Ding J, Zhao N, Shi C, Du X, Li J. In situ formation of Cu-ZrO_2 composites by chemical routes. *Journal of Alloys and Compounds.* 2006;425(1-2):390-394.
25. Gao J, Zheng J, Hou C. Nano zirconia reinforced Cu-matrix composites. *Heat Treatment of Metals.* 2006;31(1):40-42.
26. Towle DJ, Friend CM. Comparison of compressive and tensile properties of magnesium based metal matrix composites. *Materials Science and Technology.* 1993;9(1):35-41.
27. Cullity BD. *Elements of X-ray Diffraction.* 2nd ed. Boston: Addison-Wesley; 1978.
28. Slipenyuk A, Kuprin V, Milman Y, Goncharuk V, Eckert J. Properties of P/M processed particle reinforced metal matrix composites specified by reinforcement concentration and matrix-to-reinforcement particle size ratio. *Acta Materialia.* 2006;54(1):157-166.
29. Wagih A, Fathy A. Experimental investigation and FE simulation of nano-indentation on Al-Al_2O_3 nanocomposites. *Advanced Powder Technology.* 2016;27(2):403-410.
30. Wagih A, Fathy A, Sebaey TA. Experimental investigation on the compressibility of Al/Al_2O_3 nanocomposites. *International Journal of Materials and Product Technology.* 2016; 52(3-4):312-332.
31. Fathy A, El-Kady O. Thermal expansion and thermal conductivity characteristics of Cu-Al_2O_3 nanocomposites. *Materials & Design.* 2013;46:355-359.

32. Lei W, Zhu D, Qu N. Research on mechanical properties of nanocrystalline electroforming layer. *Chinese Journal of Mechanical Engineering.* 2004;40(12):124-127.

33. El-Kady O, Fathy A. Effect of SiC particle size on the physical and mechanical properties of extruded Al matrix nanocomposites. *Materials & Design (1980-2015).* 2014;54:348-353.

34. Fathy A, El Kady O, Mohammed MMM. Effect of iron addition on microstructure, mechanical and magnetic properties of Al-matrix composite produced by powder metallurgy route. *Transactions of Nonferrous Metals Society of China.* 2015;25(1):46-53.

35. Narayanasamy R, Ramesh T, Pandey KS. Workability studies on cold upsetting of Al-Al_2O_3 composite material. *Materials & Design.* 2006;27(7):566-575.

36. Fathy A, Elkady O, Abu-Oqail A. Production and properties of Cu-ZrO_2 nanocomposite produced by thermochemical process. *Journal of Alloys and Compounds.* 2017;719:411-419.

37. Fathy A, Elkady O, Abu-Oqail A. Microstructure, mechanical and wear properties of Cu-ZrO_2 nanocomposites. *Materials Science and Technology.* 2017.